Asian Journal of Green Chemistry 6 (2022) 255-272

Asian Journal of Green Chemistry

Journal homepage: www.ajgreenchem.com

Original Research Article

Analysis and detection of incident light attenuation with a continuous flow injection by using the precipitating reaction of fluconazole and phosphomolybidic acid by NAG4SX3-3D instrument

Nagham Shakir Turkie, Sarah Faris Hameed*

Department of Chemistry, College of Science, University of Baghdad, Baghdad, Iraq

ARTICLE INFORMATION

Received: 26 July 2022
Received in revised: 13 September 2022
Accepted: 16 September 2022
Available online: 3 October 2022

DOI: 10.22034/ajgc.2022.3.6

KEYWORDS

Fluconazole
Turbidity
Continuous flow Injection Analysis
Attenuation of Incident Light

ABSTRACT

A quick and sensitive approach for detecting fluconazole by formation a pale yellow precipitate from the interaction of phosphomolybdic acid and fluconazole in a sulfuric acid medium. The relevant parameter was investigated to increase the sensitivity of the newly proposed technique. L.O.D. = 16.0792 ng/sample at the lowest concentration on the calibration curve over the progressive dilution exhibited, a linear range (0.01-6) mmol.L^{-1} for fluconazole measurement, significantly lower than 0.2 RSD% for repetition (n = 6). With a linear R^2 of 99.73% and a linear dynamic range of 0.9987, (correlation coefficient). The UV-spectrophotometric at λ_{max} = 260 nm and the turbidimetric method were used as benchmarks against which to evaluate the performance of the suggested strategy. It was determined that, in comparison to the conventional method by using 10 mm irradiation, the sensitivity of the created technique, its usage of few chemicals, and its dynamic mechanism for preventing precipitated particle setting during tests all set it apart. The continual dilution of CFIA also allows for the manipulation of either high or low concentrations, thereby increasing the range of conceivable uses. Compared with the reference procedures, the developed method is thought to be the most accurate means of identifying fluconazole molecules in their purest and the most pharmaceutically effective forms.

Corresponding authors, email: sarahf.hameed@yahoo.com (S. Faris Hameed).

Graphical Abstract

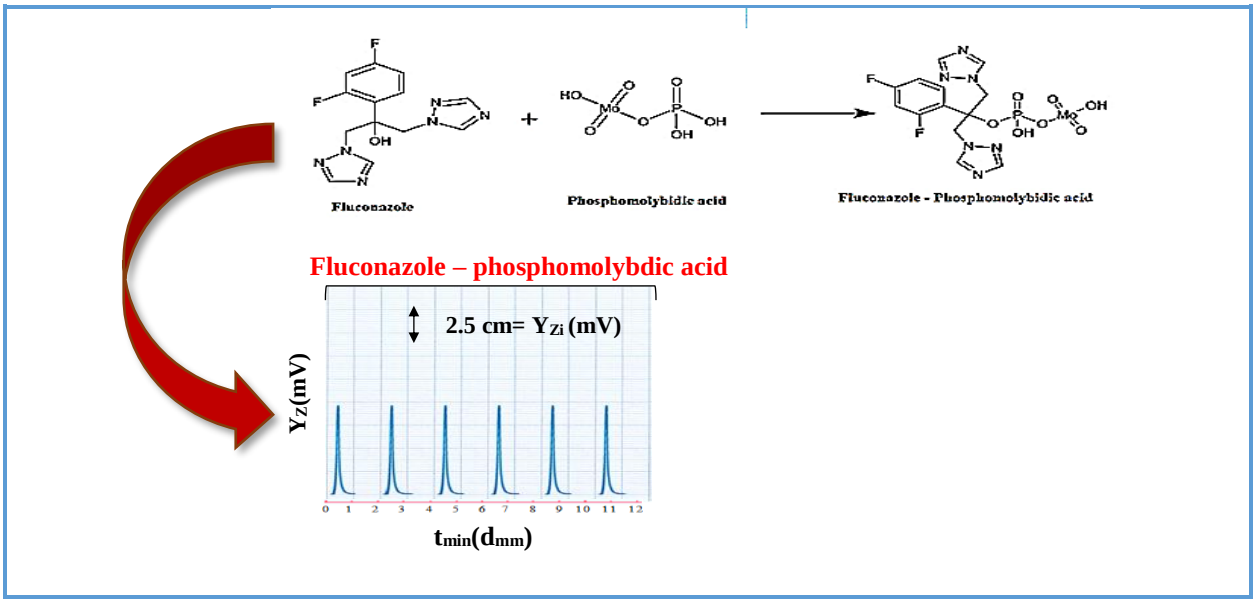

Introduction

Fluconazole is a drug (triazole) antifungal, as depicted in Scheme 1 that is used to treat superficial and systemic candidiasis, as well as cryptococci infections in individuals with acquired immunodeficiency syndromes (AIDS) [1]. It works by inhibiting the ergosterol production, a major part of the fungal cell membrane like antibiotics [2]. Fluconazole is less lipophilic than other azoles (e.g., ketoconazole, itraconazole and miconazole). It was first synthesized in 1982. The inclusion of a halogen–phenyl group boosts antifungal action and water solubility, resulting in increased bioavailability [3]. Used to protect people from getting yeast infections before a bone marrow transplant who are at risk for getting them because they are receiving chemotherapy or radiation treatment. Even today, fluconazole is frequently used to treat fungi, including C. [4] infection with albicans. Studies on fluconazole resistance mechanisms are widespread. Nevertheless, despite comprehensive awareness of these pathways, not all therapy failures may be attributed to the resistance development. Indeed, it has been discovered that several isolates that were fluconazole sensitive *in vitro* cannot be effectively treated in the patient. Some clinical isolates of C. are well-known to have C. fluconazole is more tolerated by some albicans than others. When medication concentrations are greater than their minimal inhibitory concentration, these are characterized by enhanced growth, known as residual growth [5]. There are numerous methods to determine fluconazole such as mass spectroscopy [6], Uv-spectrophotometry [7], NIR spectroscopy, and chemo metrics [8].

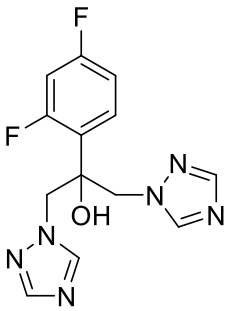

Scheme 1. The structure of fluconazole

Experimental

Materials and methods

The results from incident light attenuation from 0 to 180 degrees were collected, this experiment involved building a flow cell (the cell that the material flow in it) with a home-built NAG-4SX3-3D analyzer. The data from the output signals was recorded by using a potentiometric recorder. A peristaltic pump (Ismatec) with a sample loop and a six-way injection valve is used (Teflon, variable length). A Shimadzu UV spectrophotometric and turbidimetric equipment was used to conduct the routine operations.

The solutions were prepared with distilled water and only analytical reagent-grade ingredients were used. By dissolving 1.5314 g of fluconazole ($C_{13}H_{12}F_2N_6O$, molecular weight 306.271 g.mol^{-1}) in 250 mL of distilled water, fluconazole, with a standard concentration of 0.02 M and a molecular weight of 306.271 g.mol^{-1}, was produced. A 0.012 M standard solution was made by dissolving 5.475 g of phosphomolybidic acid ($H_3Mo_{12}PO_{40}.12H_2O$), which has a molecular weight of 1,825.25 g.mol^{-1} in 250 mL of distilled water.

Methodology

As can be seen in Figure 1, there are two distinct pathways making up the manifold strategy for identifying fluconazole in medicines. In the acidic medium, fluconazole and phosphomolybidic acid react to produce a pale yellow precipitate. A drug sample segment with a sample loop capacity of 175 µL is carried to the injection point through the first line from the manifold, which is a carrier stream of distilled water moving at a flow rate of 2.5 mL.min^{-1} and connected to an injection valve. The phosphomolybidic acid is supplied at a rate of 2.5 mL.min^{-1} (3 mmol.L^{-1}) via the second line. The mV vs. time response data is collected by a locally designed turbidimeter (NAG-4SX3-3D Analyzer) [9] when the pale yellow precipitate forms at the Y-junction of the two lines. Scheme 2 depicts a similar ion pair mechanism for Flu-PMA [10] in acidic media. The obtained results are indicated in Figure 2.

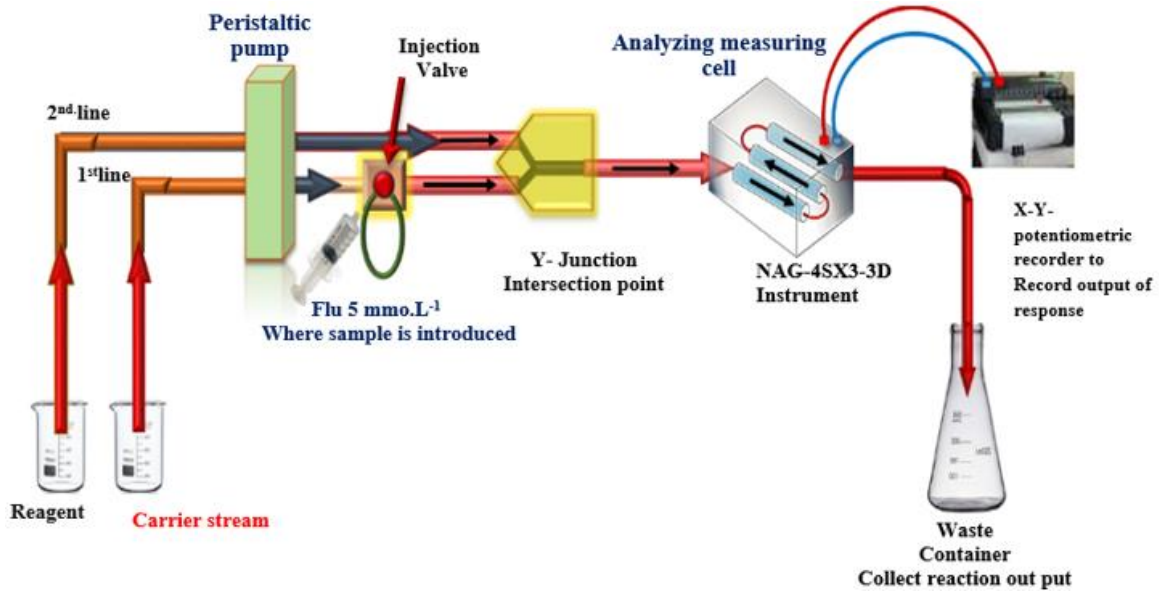

Figure 1. The design of the used manifold to estimate fluconazole

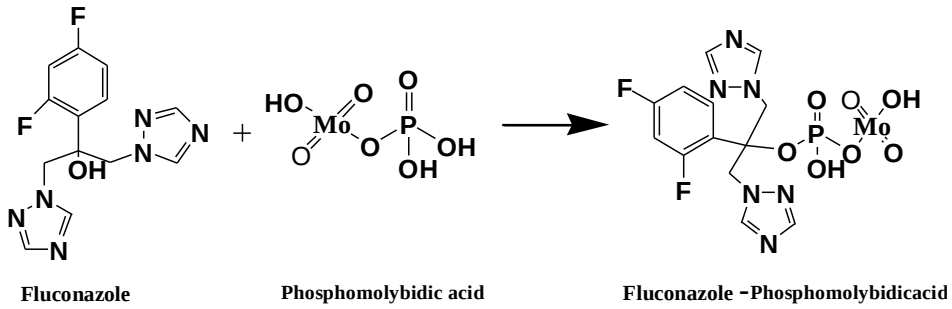

Scheme 2. The proposed reaction for fluconazole with phosphomolybidic acid system

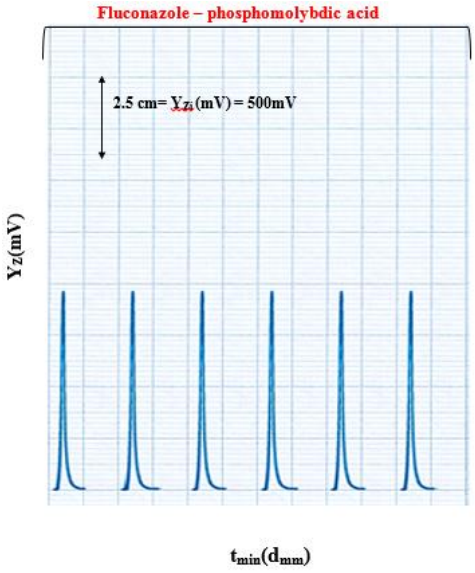

Figure 2. The continuous repeated on-line measurements

Results and Discussion

The optimal conditions for producing the reaction's ultimate result, a pale-yellow precipitate, depicts in Figure 1 employing a flow injection manifold system to provide the optimum accuracy and sensitivity. We had the most success when ignored all other variables and concentrated just on these spots for enhancement.

Chemical variables

Effect of variable concentration of phosphomolybdic acid

The stock solution is diluted with distilled water. Phosphomolybdic acid solutions with concentrations ranging from (2-8) mmol.L^{-1} were produced and carried out three times each. Figure 3 illustrates how the NAG-4SX3-3D analyzer's energy transducer response varies with phosphomolybdic acid concentration. When utilizing different concentrations of the reagent phosphomolybdic acid from (2 to 6) mmol.L^{-1}, the increased in S/N energy transducer response might be due to the dispersion of the precipitate particle as the phosphomolybdic acid concentration increased. As a consequence, 6 mmol.L^{-1} for phosphomolybdic acid was the best concentration.

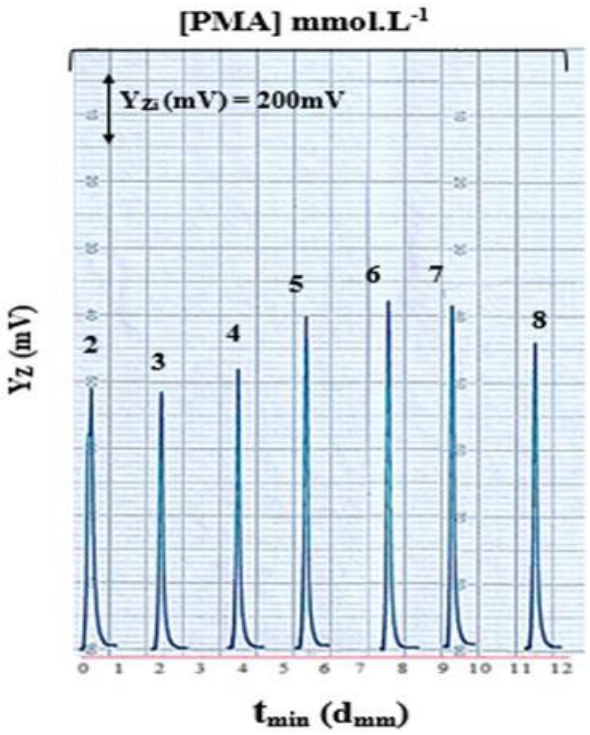

Figure 3. The reagent concentrations impact the response profile

Effect of different medium (salts and acids)

Fluconazole -phosphomolybdic acid was tasted by using the characteristics of the fluconazole system. a carrier stream was used to test the impact of different solutions. Along with the aqueous medium, the other solution media with a 50 mmol.L^{-1} concentration include CH_3COOH, tartaric acid, ascorbic acid, HCl, HNO_3, H_2SO_4, KCl, CH_3COONH_4, NH_4Cl, $NaNO_3$, NaCl, and Na_2CO_3. Figure 4 shows a reduction in S/N response caused by the tested material. This could be the outcome of the agglomeration growth or an increase in terms of density and compactness overall. All chemicals except H_2SO_4 cause the S/N response to go down. This is because H_2SO_4 creates tiny solid particles that shorten the distances between spaces and reduce the light amount that gets through. Due to the increased number of gaps between agglomerations of particle, the incident light intensity rises as a result. H_2SO_4 was selected as the optimum carrier stream for fluconazole in this investigation because it was satisfactory for the sensitivity and produced a stronger response.

Effect of H_2SO_4 concentration

From 30 to 150 mmol/L of H_2SO_4 were produced as solutions. An open valve mode was employed. Each experiment was carried out three times and the results indicated that the attenuation of incoming light rose as the concentration of H_2SO_4 did. This was due to the nucleus-like morphology of some microscopic particles, which helped them clump together into dense blocks. More than 100 mmol.L^{-1} of incident light will be attenuated, and micro size solubility will rise as a result. It was found that a carrier stream of 100 mmol.L^{-1} H_2SO_4 worked best, as shown in Figure 5.

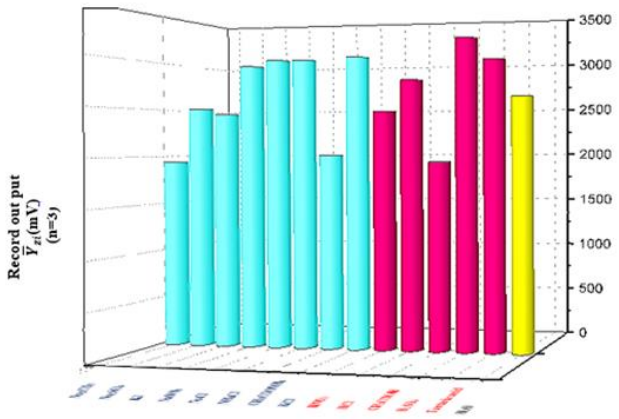

Figure 4. The effect of different medium

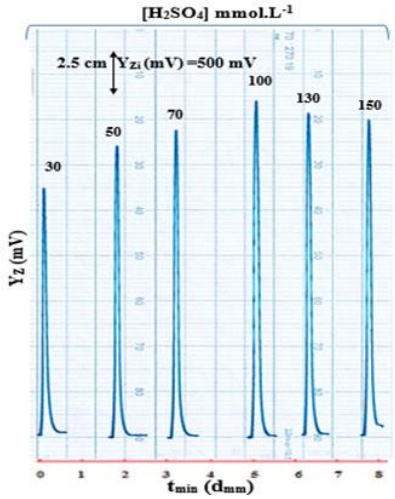

Figure 5. Effect of different concentrations of sulfuric acid on the response

Physical variables

Flow rate

The peristaltic pump was used to adjust the flow rates of the carrier stream and reagent for the fluconazole detection at 5 mmol.L^{-1}. As demonstrated in Figure 6, 2.5 mL.min^{-1} of flow rate was selected for the carrier and reagent lines as an adequate flow rate for this particular project, despite the fact that a higher flow rate (<2.5 mL.min^{-1} for the carrier stream and reagent) decreased sensitivity and resulted in a broader base of response (increase Δt_B).

Sample volume

Variable sample volumes were used with open valve mode. Figure 7 displays that 175 µL was the best sample volume for fluconazole, which is characterized by sharpness and a smooth response profile, as well as economy and reduced analysis time. Up to the sample volume of 175 µL for fluconazole as sample volume grew, so did the peak of the reaction, but the response profile remained unchanged. There was a continuous growth in peak maxima as the volume was increased to over 175 µL. The effects are illustrated in Figure 7.

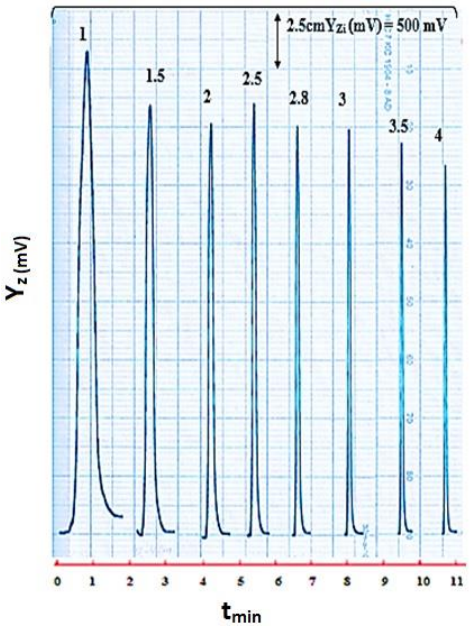

Figure 6. The influence of flow rate in mL.min^{-1}

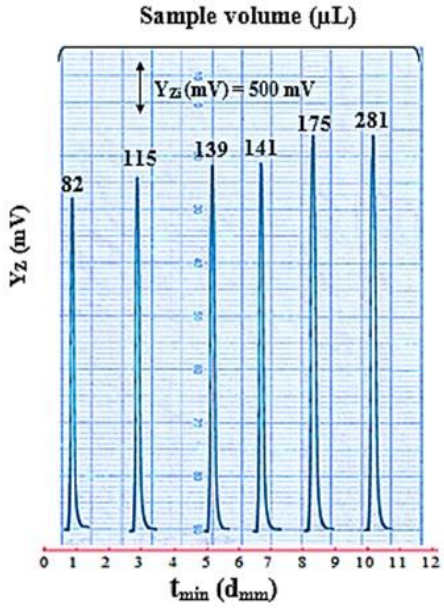

Figure 7. The sample volume response profile to the energy transducer response when fluconazole was detected by using the NAG-4SX3-3D analyzer

Effect of reaction loop lengths

The system utilized was fluconazole (5.0 mmol.L^{-1}), phosphomolybdic acid (6.0 mmol.L^{-1}), and sulfuric acid (100 mmol.L^{-1}). There was a look at how much of a role the reaction coil plays. How long a reaction coil is plays a role in how well and how completely chemical reactions are carried out. We used coils of varying lengths (from 0 to 30 cm) and volumes (from 0 to 942 µL), which were all connected in series through the Y-junction of the fluid system

(Figure 8 and Table 1). Other factors, such as base width (Δt_B), widening at peak maxima, and the departure time for sample segment from injection valve to measure cell are also responsible. This may be because of the continuously increasing effect of dilution and dispersion on the precipitated segment and the continuously longer time duration of precipitate species in front of the detector.

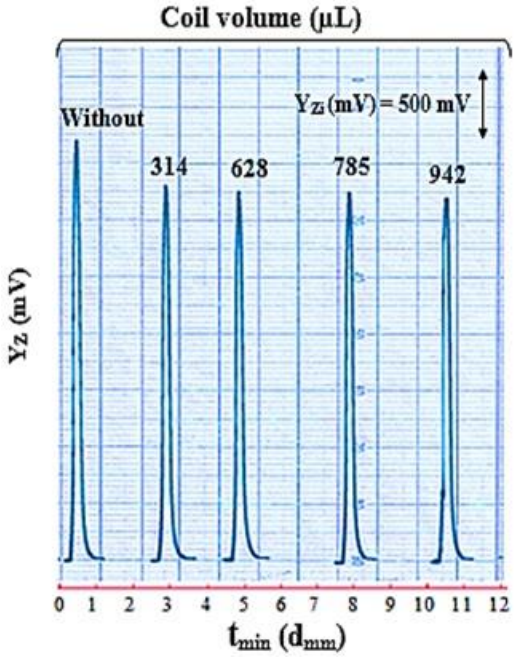

Figure 8. The response of coil volume in different volumes

Table 1. Variation effect of the reaction coil on precipitation of fluconazole

Coil length Cm r=1 mm	Coil length µL	$\bar{Y}_{Zi}$(mV) average (n=3)	RSD %	Δt_B Sec	V_{add} (mL) at flow rate	C (mmo.L^{-1})	D.F	Confidence interval at 95% $\bar{Y}_{Zi}$(mV)± t SEM	t_{sec}
Without	0	3760	0.09	36	3.175	0.276	18.1429	3760±8.645	12
10	314	3320	0.14	42	3.675	0.238	21.0000	3320±11.229	15
20	628	3260	0.15	45	3.925	0.223	22.4286	3260±12.372	18
25	785	3260	0.15	48	4.175	0.210	23.8571	3260±12.397	21
30	942	3180	0.16	51	4.425	0.198	25.2857	3180±12.943	24

$\bar{Y}_{Zi}$(mV):(S/N) energy transducer response in m.

Study of Y-junction point

In the process, the Y-junction is required for reactant mixing. Before measuring the cell directly in the flow system, the Y-junction was attached. The effect of changing the Y-junction in different parameters on the response profile was explored. In Figure 9, we can see how the Y-junction is affected by the energy response of the S/N transducer. Particle agglomeration, regulation, and regular distribution were tested with a series of mixing chambers of varying volumes and a larger diameter at the point where they entered the flow tube. However, as interspatial distances increase and particle scattering and dispersion diminish our ability to block incoming light from increasing the energy transducer, in Figure 10, the height of response measurement as a manifold unit with two 3 mm

(I.D.) entry and a 3 mm (I.D.) output was, therefore, suggested as a possible solution for removing the premix chamber or junction point. The information provided here suggests that the reactant mixing and the formation of precipitate particles in a sulfuric acid medium can occur without the use of a Y-junction.

A scatter plot is used to estimate the linear dynamic range for fluconazole's effect on S/N energy transducer response variation

With established optimal parameters, a collection of fluconazole solutions starting from 0.001to 13 mmol.L^{-1} were created.

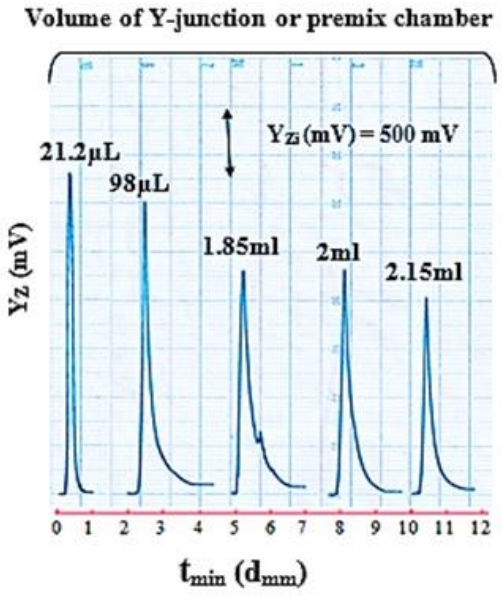

Figure 9. Response profile of Yz (mV) - $t_{min}(10_{mm})$ for the determination of fluconazole using NAG-4SX3-3D analyzer via the formation of pale yellow precipitate of fluconazole

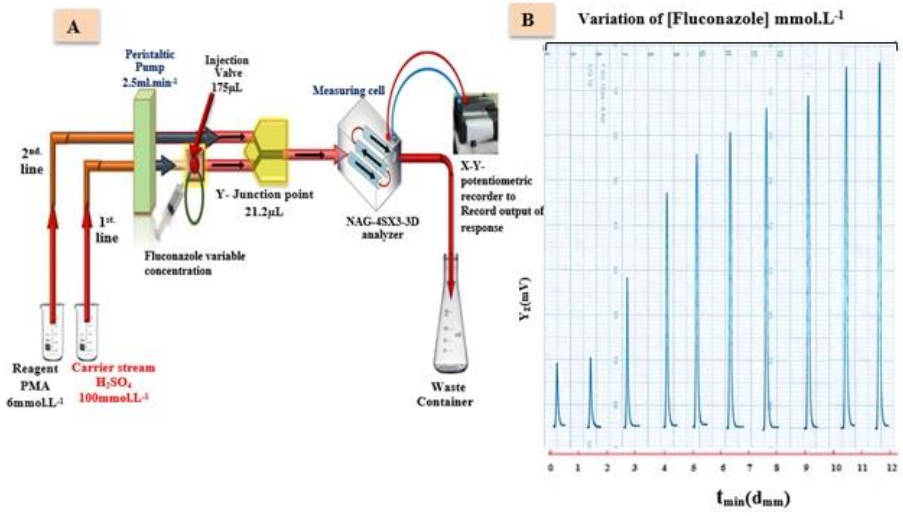

Figure 10. A) A system used to measure fluconazole, B) Some time-based profiles and potentiometric scanning speed 1 cm.min^{-1}

Figure 10**a** displays the response profile for this experiment. The linear calibration graph range for the fluctuation of the energy transducer response of the NAG-4SX3-3D Analyzer with fluconazole concentration was (0.001-6) mmol.L^{-1}, according to a scatter plot diagram (Figure 10**b**). With a correlation value (r) of 0.9989, the height of the response grew as the analyte concentration rose until it reached 10 mmol.L^{-1}. Figure 11 illustrates the variance ranges for the system (i.e. the scatter plot (0.001- 13) mmol.L^{-1}, dynamic range (0.001-10) mmol.L^{-1}, and working range (0.001-8) mmol.L^{-1}. The obtained results are presented in Table 2.

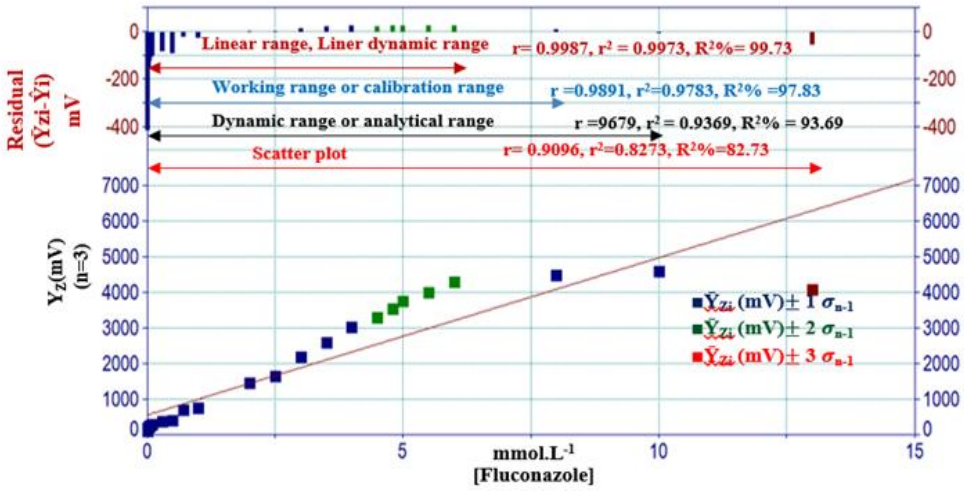

Figure 11. Influence of fluconazole concentration on the response

Table 2. Results of linear regression to determine how the (S/N) energy transducer response varies with Fluconazole concentration

Types of range	Range of [Fluconazole] mmol.L^{-1} (n)	$\hat{Y}_{Z\,i}=a \pm S_a\,t+b(\Delta y/\Delta x_{mmol/L}) \pm S_b\,t$ [Flu] mmol.L^{-1}	r, r^2, R^2%	t_{tab} at 95% , n-2	Calculated t-value $t_{cal}=/r/\sqrt{n-2}/\sqrt{1-r^2}$
Linear range	0.001-6 (22)	159.2634±48.754+697.662±16.863 [Fluconazole]	0.999, 0.997, 99.70	2.086	<<86.302
Working range	0.001-8 (23)	226.4352±142.759+643.651±43.484 [Fluconazole]	0.989, 0.978, 97.80	2.080	<<30.787
Dynamic range	0.001-10 (24)	347.6574±245.954+562.896±64.601 [Fluconazole]	0.968, 0.937, 93.70	2.074	<<18.072
Scatter plot	0.001-13 (25)	567.4682± 395.506+441.263±86.981 [Fluconazole]	0.910, 0.827, 82.70	2.69	10.496

Table 3. Detection limit of fluconazole-phosphomolybdic acid-H_2SO_4 (100 mmol/L) system

Practically		Theoretical $x=3S_B/slope$	Theoretical $\hat{Y} = Y_b + 3Sb$	L.O. Q [13]
Pioneered approach (0.0003) mmol	Traditional approach UV-method (0.0003) mmol/L Turbidmetric approach (0.005) mmol/L			
16.0792 ng/sample	0.0919 µg/sample 21.4389 µg/sample	0.2134 µg/ sample	18.4053 µg/ sample	61.3511 µg/ sample

Detection limit (LOD)

Fluconazole's detection limit was found by using three approaches: By using a scatter plot's lowest concentration as a starting point, both practically and theoretically, one can utilize the progressive dilution [11, 12]. Via phosphomolybdic acid as a precipitant, Table 3 lists the estimation of the detection limit for fluconazole.

Repeatability

The measurement's repeatability was compared with the relative standard deviation expressed as a percentage [14, 15]. At a constant fluconazole concentration, a set of six injections were measured. Fluconazole was administered at two different concentrations (2.5 and 13 mmol.L^{-1}). As demonstrated in Figure 12, the relative standard deviation was less than one percent.

Classical methods

A newly devised methodology the NAG-4SX3-3D analyzer for the fluconazole detection by using precipitating agents, phosphomolybdic acid, was compared with the prior published approaches, including UV-spectrophotometric [16] and turbidimetric methods.

A spectrophotometric technique employing a quartz cell to measure absorbance in the range of 0.001- 2 mmol.L^{-1} at λ_{max} = 260 nm. The scatter plot in Figure 13**a** displays the UV spectrum of fluconazole at 260 nm, Figure 13**b** shows that the optimum linear range is between 0.001 and 1 mmol.L^{-1}, with a correlation value of 0.9986 and an R^2 % of 99.73 % (n=16) (the number of measurement). 0.0003 mmol.L^{-1} (0.3 mol.L^{-1} corresponding to 0.0919 g/sample) was the detection limit.

Fluconazole interaction with PMA (2 mmol.L^{-1}) concentration is used in the turbidimetric approach. The scatter plot in Figure 14**a** shows that the PMA system's appropriate linear range is (0.01-1) mmol.L^{-1}, with a correlation coefficient of 0.9869 and an R^2 % of 97.72 (n= 13). (Number of measurement). The system's scatter plot was depicted in Figure 14**b** and the system's results were summarized in Table 4. The detection limit was 0.007 mmol.L^{-1} (7 µmol.L^{-1} and 21.4389 µg/sample).

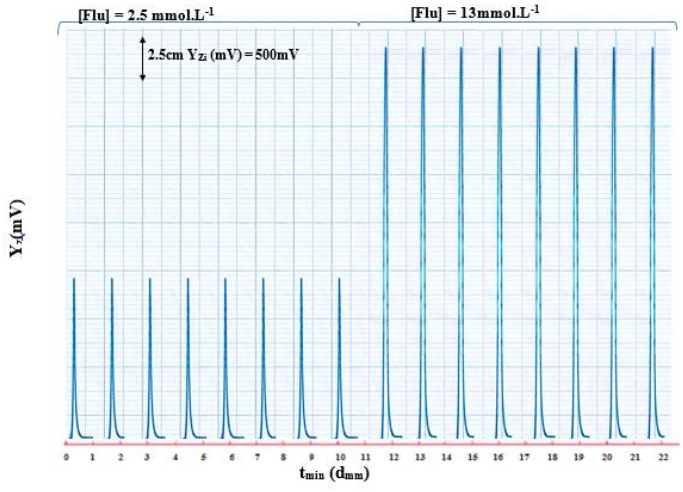

Figure 12. Profile of eight successive readings with repeatability for 2.5 mmol.L^{-1} and 13 mmol.L^{-1} concentrations of Fluconazole

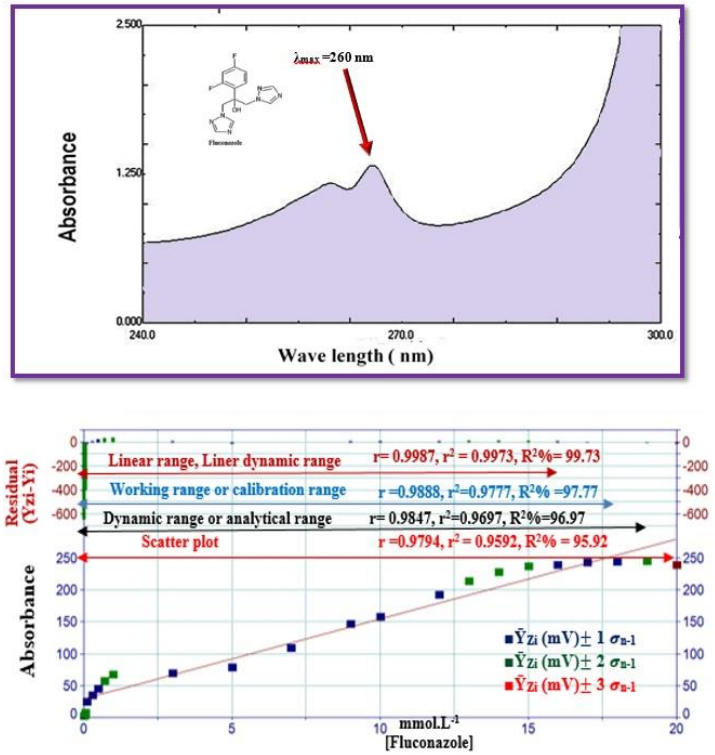

Figure 13. A) Absorbance of UV-spectrum of fluconazole 0.0003 mmol.L^{-1} at λ_{max} = 260 nm, B) The scatter plot via [Fluconazole] by utilizing the traditional technique at λ_{max}=260 nm (0.001-2) mmol.L^{-1}, n=20

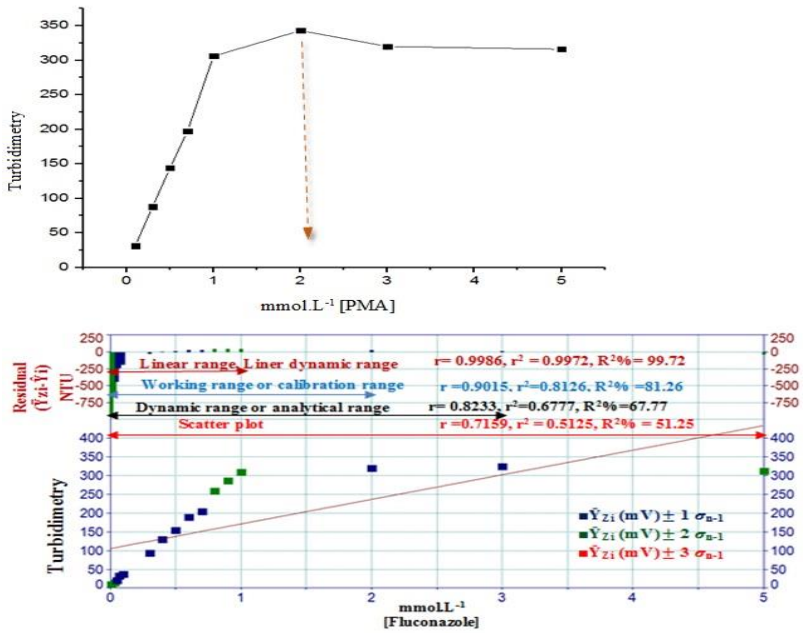

Figure 14. A) The optimal PMA concentration utilized in the turbidimetric approach is displayed graphically, B) [Fluconazole turbidimetric]'s technique scatter plot

Table 4. Fluconazole concentration ranges vs. absorbance and scatter light by using spectrophotometer and turbidimetry methods (classical methods)

Type of mode	Range of [Flu] mmol.L^{-1}(n)	$\hat{Y}_{Z\,i}=a \pm S_a\,t+b(\Delta y/\Delta x_{mmol/L}) \pm S_b\,t$ [Flu] mmol.L^{-1}	r, r^2, R^2%	t $_{tab}$ at 95%, n-2	Calculated t-value $t_{cal}=/r/\sqrt{n-2}/\sqrt{1-r^2}$
UV- Spectrophotometer at λ_{max}= 260 nm Turbidity					
Linear range	0.001-1 (16)	0.083±0.026+1.694±0.052 [Fluconazole]	0.999,0.997, and 99.70	2.145<< 7.124	
	0.01-1(13)	5.992±5.806+304.963±10.712 [Fluconazole]	0.999,0.997, and 99.70	2.201 << 62.664	
Working range	0.001-1.3 (17)	0.117±0.072+1.546±0.128 [Fluconazole]	0.989,0.978, and 97.70	2.131 << 3.383	
	0.01-2 (14)	45.049±43.338+191.999±57.992 [Fluconazole]	0.902,0.813, and 81.30	2.179 << 7.214	
Dynamic range	0.001-1.5 (18)	0.152±0.102+1.408±0.155 [Fluconazole]	0.979,0.959, and 95.90	2.120 << 3.180	
	0.01-3 (15)	75.224±52.676+120.424±49.747 [Fluconazole]	0.823,0.678, and 67.80	2.160 << 5.229	
Scatter plot	0.001-2 (20)	0.240±0.155+1.131±0.181[Fluconazole]	0.952, 0.906, and 90.60	2.101 << 3.262	
	0.01-5(16)	105.365±59.292+65.599±36.675 [Fluconazole]	0.716,0.513, and 51.30	3.837	

Determination of fluconazole in drugs by using NAG-4SX3-3D analyzer

Four pharmaceutical samples were analyzed for fluconazole by using the cutting-edge NAG-4SX3-SD analyzer. Two techniques were used in tandem with the continuous flow injection analysis via NAG-4SX3-3D analyzer: The UV measurement of absorbance at max=260 nm and turbidimetric measurement at 0-180° for the pale-yellow precipitate. We employed all three measuring techniques, and then utilized the standard addition procedure to analyze the data (Figure 15). The NAG-4S3-3D analyzer, an absorbance spectrophotometer, and the turbidimetric method were utilized. The (t-test) (Figure 16), which compares two main paths, and Table 5 show the practical content of an active component at the 95 percent confidence level and determination efficiency. Table 5 compares the created technique NAG-4SX3-3D analyzer with the officially declared amount (150 mg) by the initial computing t values [17] for each individual company and comparing them to tabulated t-values. The observed result demonstrated that the mean value and the cited value were significantly different. Following the establishment of this groundwork, the developed method can be used in the same way as the conventional addition techniques. When the calculated t-value is less than the tabulated t-value, it means that the created approach is statistically indistinguishable from the mentioned method by the company. These results show a major discrepancy between the mentioned and observed concentrations of the active component. Once this groundwork is laid, the generated method can be used in the same way as the conventional addition techniques. There are no substantial inconsistencies between the manufactured approach and the declared way by the corporation, as the computed t-value is smaller than the tabulated t-value. By using a paired t-test with a significance threshold of 0.05 (2-tailed), the NAG-4SX3-3D analyzer's results were

compared with those from the UV-spectrophotometric method by using Shimadzu (double beam UV-1800) spectrophotometry and turbidity with a turbidity meter (HANNA, Hungary). Attenuation of incident light is measured from 0 to 180 degrees and is presented in Table 6. We assume that drugs from different companies are all part of the same population and disregard any distinctions between them. The data demonstrate that at the 5% significance level, there was no statistically significant difference between the developed methodology and the UV-spectrophotometric method, or the turbidity method, both of which are regarded as more traditional methods. The results are displayed in Table 6.

A one-way ANOVA (F-test) treatment was used by the researchers, which just has one variable but compares three or more means. To measure fluconazole in various pharmaceuticals, the NAG4SX3-3D analyzer was evaluated and contrasted with three conventional techniques (the official technique, turbidity, and the UV-spectrophometric method) (Figure 17 and Table 7) [18].

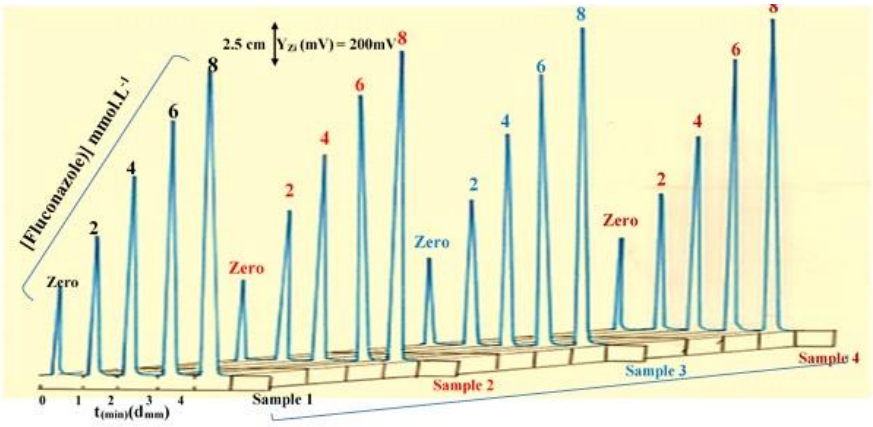

Figure 15. Using four distinct companies, the profile-time for the common addition approach for the fluconazole-phosphomolybdic acid system

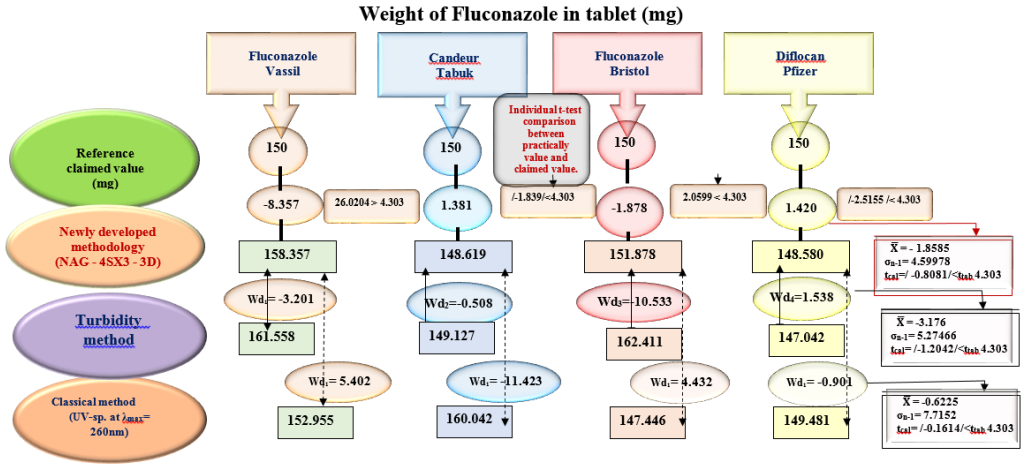

Figure 16. Individual t-test results and comparisons among newly created methodology, the turbidity method, and the UV reference method were used to compare the results between practically content and the claimed valve

Table 5. Data were achieved for the Fluconazole determination in four different models by using the NAG-4SX3-3D analyzer and two conventional techniques

No. of sample	Commercial Name, Company Content Country	Confidence Interval For Tablet's Average Weight$\bar{w}i \pm 1.96\ \sigma_{n-1}/\sqrt{n}$ at 95% (g)	Sample weight was identical to 0.1531 gm (10 mmol.L^{-1}) of the active ingredient	95 % of the active ingredient's theoretical content (mg) $Wi \pm 1.96\ \sigma_{n-1}/\sqrt{n}$	Kind of approach Newly approach Traditional turbidity UV- at λ_{max}= 260nm.	[Flu] mmol.L^{-1}					r, r^2 R^2%
					0 mL 0 mmol.L^{-1}	0.5 mL 1 mmol.L^{-1}	1.0 mL 2 mmol.L^{-1}	1.5 mL 3 mmol.L^{-1}	2.0 mL 4 mmol.L^{-1}	
					0 mL 0 mmol.L^{-1}	0.3 mL 0.6 mmol.L^{-1}	0.35 mL 0.7 mmol.L^{-1}	0.4 mL 0.8 mmol.L^{-1}	0.45 mL 0.9 mmol.L^{-1}	
					0 mL 0 mmol.L^{-1}	0.025 mL 0.05 mmol.L^{-1}	0.05 mL 0.1 mmol.L^{-1}	0.15 mL 0.3 mmol.L^{-1}	0.25 mL 0.5 mmol.L^{-1}	
1	Fluconazole Vassil 150 mg Bulgaria	0.2019±0.0230	0.2061	150±17.1173	1100 30 0.240	1760 228 0.292	2500 260 0.391	3200 286 0.814	3840 305 1.232	1.000, 1.000, 100.00 0.998, 0.996, 99.60 0.999, 0.998, 99.80
2	Candeur Tabuk 150 mg Saudi Arabia	0.2992±0.0071	0.3055	150±3.5811	1000 32 0.235	1900 222 0.329	2620 250 0.442	3360 289 0.934	3950 317 1.302	0.997, 0.995, 99.50 0.999, 0.999, 99.90 0.998, 0.997, 99.70
3	Fluconazole Bristol 150 mg UK	0.3573±0.0055	0.3648	150±2.3039	1100 33 0.169	1820 245 0.348	2680 270 0.462	3420 302 0.889	4000 330 1.298	0.998, 0.996, 99.60 0.999, 0.998, 99.80 0.998, 0.995, 99.50
4	Diflucan Pfizer 150 mg France	0.3464±0.0041	0.3536	150±1.7823	1150 38 0.183	1730 235 0.244	2470 280 0.349	3440 324 0.684	3950 355 1.038	0.996, 0.991, 99.10 0.998, 0.999, 99.90 0.999, 0.999, 99.90

Table 6. Individual t-tests comparing weight averages to quoted values for the fluconazole-phosphomolybidic acid system and a summary of the system's practical content and efficiency (Rec percent) in identifying fluconazole in four product samples

No. of sample	Practical concentration (mmol.L^{-1}) in 10 ml Practical concentration (mmol.L^{-1}) In50 ml Practical weight of Flu. in (g)	Newly approach Traditional turbidity UV at λ_{max}= 260 nm. Weight of Flu in each sample (g) $\bar{W}_{i(g)} \pm 4.303\ \sigma_{n-1}/\sqrt{n}$ Weight of Flu in tablet $\bar{W}_{i(mg)} \pm 4.303\sigma_{n-1}/\sqrt{n}$	Efficiency of determination Rec.%	Individual t-test between claimed value & practical value ($\bar{W}_{i(mg)}$-μ) $\sqrt{n}$ /σ_{n-1}	Paired t-test Compared between three methods t_{cal}= $\bar{w}d\sqrt{n}/\sigma^{*}_{n-1}$	t_{tab} at 95%confidence level (n-1)
1	1.5838 10.559 0.1617	0.15836±0.0013 158.357±1.328	105.57	26.0204>> 4.303	Newly developed methodology + quoted value (reference method) ---------- - $\bar{X}d$ = - 1.8585 σ^{*}_{n-1} = 4.5998 /-0.8081/ <4.303	
	0.1077 10.772 0.1649	0.161558±0.0043 161.558±4.325	107.71			
	0.1020 10.1990 0.1562	0.15295±0.0020 152.955±1.982	101.97			
	1.4864 9.9094 0.1518	0.148619±0.0032 148.619±3.231	99.08			
2	0.0994 9.9433 0.1523	0.149126±0.0023 149.127±2.348	99.42	/-1.839/ < 4.303	Newly developed methodology and UV-(traditional method) ---------- $\bar{X}d$ = - 0.6225 σ^{*}_{n-1} = 7.7152 /-0.1614 / <4.303	
	0.1067 10.6710 0.1634	0.160042±0.0040 160.042±3.982	106.69			
	1.5189 10.1261 0.1551	0.151878±0.0039 151.878±3.923	101.25			
3	0.1083 10.8283 0.1658	0.16241±0.0043 162.411±4.324	108.274	2.0599 < 4.303		
	0.0983 9.8306 0.1505	0.14745±0.0028 147.446±2.832	98.297		Newly developed methodology and turbidity (classical method) ---------- $\bar{X}d$ = - 3.176 σ^{*}_{n-1} = 5.27447 /- 1.2042/ <4.303	
	1.4856 9.9042 0.1517	0.148580±0.0024 148.580±2.429	99.05			
4	0.0980 9.8017 0.1501	0.14704±0.0035 147.042±3.482	98.028	/-2.5155/<4.303		
	0.0996 9.9643 0.1526	0.14948±0.0020 149.481±1.987	99.65			

Table 7. The results of an analysis of variance test were used to compare four models of four different sellers

Source	(SSq)	Df	(MSq)	F_{cal}	$F_{critical}$
Between groups	SS_B=98.47329	3	MS_B=32.82443	1.2938<3.490295	
Within groups	SS_W=304.4430	12	MS_W=25.37025		
Total	402.9163	15			

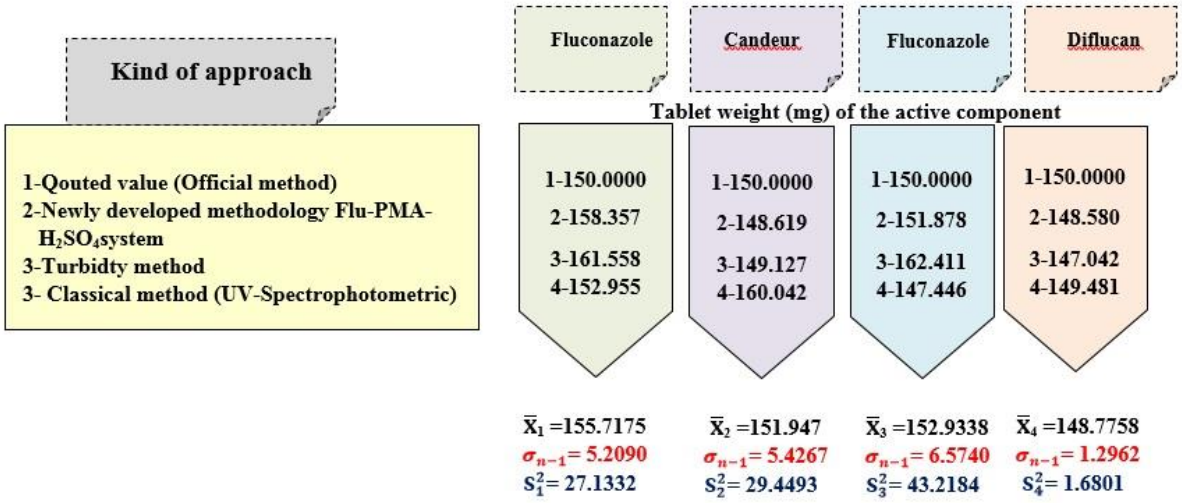

Figure 17. The consolidated data from three independent, in addition to the referenced value, and four independent samples used in the ANOVA

Conclusion

The recommended procedure uses cheaper equipment and chemical ingredients than the standard procedures. The NAG-4SX3-3D analyzer was used to produce a faster and more accurate result. The repeated standard deviations (RSD%) (n = 6) were significantly lower than 0.2%, proving the accuracy of the suggested method. Furthermore, this technique has the potential to be employed in fluconazole evaluation, and it has the benefit of the great sensitivity without the requirement for heat or extraction. The statistical findings were consistent with those obtained by more conventional means.

Disclosure Statement

No potential conflict of interest was reported by the authors.

Orcid

Sarah Faris Hameed 0000-0002-7607-3498

References

[1]. Mohamed A.Z., Manal A.E., Marwa A.A. *Egypt. J. Chem*., 2017, **60**:1177 [Crossref], [Google Scholar], [Publisher]

[2]. Marcio L.R. *mBio*, 2018, **9**:e01755-18 [Crossref], [Google Scholar], [Publisher]

[3]. Lakhani P., Patil A., Majumdar S. *Journal of Ocular Pharmacology and Therapeutics*, 2019, **35**

[4]. Berman J., Krysan D.J. *Nature Reviews Microbiology*, 2020, **18**:319 [Crossref], [Google Scholar], [Publisher]

[5]. Kim J.Y. Journal of Microbiology, 2016, **54**:145 [Crossref], [Google Scholar], [Publisher]

[6]. Urszula H., Jan K., Pawe£ Q.Q.W., Dariusz M., Agata K. *Acta Poloniae Pharmaceutica ñ Drug Research*, 2019, **76**:19ñ27 [Crossref], [Google Scholar], [Publisher]

[7]. Dinesh B.K., Hina M.Y., Swapnil R.P. *Am. J. PharmTech Res*., 2020, 10:83 [Crossref], [Google Scholar]

[8]. Rodionov O.Y., Titova A.V., Demkin N.A., Balyklova K.S., Pomerantsev A.L. *Talanta*, 2019, **195**:662 [Crossref], [Google Scholar], [Publisher]

[9]. Sarah F.H., Nagham S.T. *Eurasian Chem. Commun*., 2022, **4**:790 [Crossref], [Google Scholar], [Publisher]
[10]. Sharmin E., Zafar F. Spectroscopic Analyses-Developments and Applications. 2017 [Crossref], [Google Scholar], [Publisher]
[11]. VirgÃ-lio A., Silva A.B.S., Nogueira A.R.A., Nobrega J.A., Donati G.L. *Journal of Analytical Atomic Spectrometry*, 2020, **35:**1614 [Crossref], [Google Scholar], [Publisher]
[12]. Lavín Á., Vicente J., Holgado M., Laguna M.; Casquel R., Santamaría B., Maigler M., Hernández A., Ramírez Y. *Sensors*, 2018, **18**:2038 [Crossref], [Google Scholar], [Publisher]
[13]. *Anal. Methods*., 2020, **12:401** [Crossref], [Google Scholar], [Publisher]
[14]. Kallner A., Theodorsson E. *Scandinavian Journal of Clinical and Laboratory Investigation*, 2020, **80**:210 [Crossref], [Google Scholar], [Publisher]
[15]. Wylde Z., Bonduriansky R. *Ecology and Evolution*, 2021, **11**:763 [Crossref], [Google Scholar], [Publisher]
[16]. Shoaeb M.S., Marathe R. *Pharmaceutical and Biosciences Journal*, 2020, **8**:22 [Crossref], [Google Scholar], [Publisher]
[17]. Prabhaker M., Uttam S., Chandra M.P., Priyadarshni M., Gaurav P. *Ann Card Anaesth*., 2019, **22**:407 [Crossref], [Google Scholar], [Publisher]
[18]. Kim T.K. *Korean Journal of Anesthesiology*, 2017, **70**:22 [Crossref], [Google Scholar], [Publisher]

How to cite this manuscript: Nagham Shakir Turkie, Sarah Faris Hameed*. Analysis and detection of incident light attenuation with a continuous flow injection by using the precipitating reaction of fluconazole and phosphomolybidic acid by NAG4SX3-3D instrument. *Asian Journal of Green Chemistry*, 6(3) 2022, 255-272. DOI: 10.22034/ajgc.2022.3.6